HHS Public Access

Author manuscript

Bioanalysis. Author manuscript; available in PMC 2015 December 01.

Published in final edited form as:

Bioanalysis. 2015 ; 7(3): 353–371. doi:10.4155/bio.14.306.

Protein dielectrophoresis and the link to dielectric properties

Fernanda Camacho-Alanis[*,1] and **Alexandra Ros**[1]

[1]Department of Chemistry & Biochemistry, Arizona State University, Tempe, AZ, USA

Abstract

There is a growing interest in protein dielectrophoresis (DEP) for biotechnological and pharmaceutical applications. However, the DEP behavior of proteins is still not well understood which is important for successful protein manipulation. In this paper, we elucidate the information gained in dielectric spectroscopy (DS) and electrochemical impedance spectroscopy (EIS) and how these techniques may be of importance for future protein DEP manipulation. EIS and DS can be used to determine the dielectric properties of proteins predicting their DEP behavior. Basic principles of EIS and DS are discussed and related to protein DEP through examples from previous studies. Challenges of performing DS measurements as well as potential designs to incorporate EIS and DS measurements in DEP experiments are also discussed.

Proteins are essential for life. As enzymes they catalyze chemical reactions and in cell membranes they build ion channels and pumps; they are responsible for signal generation and transmission and they also act as antibodies, hormones, toxins, antifreezing agents, elastic fibers or source of luminescence among other functions. The development of an efficient, fast and economical purification, separation and identification method of proteins is of great interest in many fields such as fabrication of pharmaceuticals, in diagnostics but also in therapy [1]. Great efforts are being devoted to the development of separation techniques for the concentration, separation and identification of these macromolecules. Standard chromatography and electrophoresis based techniques are well-established routine methods for the separation of proteins. However, conventional separation techniques reach their limitations for increased sample complexity demanding for the analysis of relevant disease markers in extremely small concentration and within a huge background [2]. A novel technique such as dielectrophoresis (DEP) can be used as an alternative to the traditional protein purification and separation methods for proteins, since DEP can achieve manipulation of biomolecules in gel-free environment as well as rapid separation and preconcentration capability [2-4]. In addition, performing these processes in microfluidic systems allows handling of nanoliter volumes, different processing steps without sample transfer, short analysis time achieved by reduction of length scales without loss of efficiency, a high degree of parallelization, high-throughput processing and process automation [5,6]. Furthermore, performing DEP on microfluidic platforms allows generating

[*]Author for correspondence: Tel.: 480 965 2175, Fax: 480 965 7954, facamach@asu.edu.

Financial & competing interests disclosure: The authors have no other relevant affiliations or financial involvement with any organization or entity with a financial interest in or financial conflict with the subject matter or materials discussed in the manuscript apart from those disclosed.

No writing assistance was utilized in the production of this manuscript.

high electric field gradients, which are essential to induce DEP forces. A wide variety of designs [6-8], thanks to the use of microfabrication techniques, have allowed the integration of tailored geometries and electrodes in size and spacing suitable to achieve large electric field gradients.

DEP is the migration of polarized particles in an inhomogeneous electric field ($\overrightarrow{E}$). The direction of particle movement depends on the real part of the Clausius–Mossotti factor, Re[$f_{CM}(\omega)$], as shown in Equation 1:

$$Re[f_{CM}(\omega)]=\left(\frac{\varepsilon_p^*-\varepsilon_m^*}{\varepsilon_p^*+2\varepsilon_m^*}\right) \quad \text{Equation 1}$$

where ε_m^* and ε_p^* are the complex permittivity of the medium and the particle. The complex permittivity is given by $\varepsilon^*=\varepsilon-j\frac{\sigma}{\omega}$, where σ is the conductivity, ω is the frequency and $j=\sqrt{-1}$. The DEP force $\overrightarrow{F}_{DEP}$ exerted on a suspended spherical particle depends on the particle radius (r), the strength of the electric field gradient ∇E^2 and Re[$f_{CM}(\omega)$] as follows:

$$\overrightarrow{F}_{DEP}=2\pi\varepsilon_m\varepsilon_0 r^3 Re[f_{CM}(\omega)]\nabla E^2 \quad \text{Equation 2}$$

where ε_m and ε_0 are medium and vacuum permittivity, respectively.

Particles are either attracted to the regions of highest electric fields or repulsed from those regions depending on the sign of the Re[$f_{CM}(\omega)$] factor. If the permittivity of the particle is greater than that of the medium ($\varepsilon_p^*>\varepsilon_m^*$), the DEP is referred to as positive DEP (pDEP). Negative DEP (nDEP) occurs when the $\varepsilon_p^*<\varepsilon_m^*$, as schematically represented in Figure 1. At high frequency, $\overrightarrow{F_{DEP}}$ is typically governed by the particle permittivity. At low frequency and under DC conditions the Re[$f_{CM}(\omega)$] is dominated by the conductivity of the particle (σ_p) and the medium (σ_m); therefore, Equation 2 can be written in terms of conductivities. Additionally, the crossover frequency is defined as the frequency under which the Re[$f_{CM}(\omega)$] reverses its sign.

Proteins are nanoscale biomolecules and require the generation of large electric field gradients in the order of 10^{17}–10^{21} V^2/m^3 [2,9–11], posing stringent requirements on the devices suitable to manipulate proteins by DEP. Consequently, micro- and nanoscale fabrication of electrodes and devices have been developed to generate sufficiently large electric field gradients. In most cases, these are embedded in some sort of fluidic environment. Such miniaturized fluidic devices or lab-on-a-chip (LOC) devices can integrate several additional operations within a microfluidic platform such as injection and detection, which could be directly exploited in an analytical sense. LOCs also gained enormous interest for protein manipulation and analysis due to their high flexibility of design, low sample consumption, rapid analysis time and minimization of manual handling steps. Therefore, there is a growing interest in the development of LOC devices with protein DEP capabilities.

DEP may interplay with other effects. Electrokinetic effects as well as diffusion of the particles have to be considered since they may counteract the DEP force. The electrokinetic flow, which is proportional to the electric field, comprises the effects of electroosmosis and electrophoresis. Electroosmotic flow is the movement of bulk liquid when a DC electric field is applied in a microchannel on particle motion relative to charged channel walls. In contrast, electrophoresis is the movement of charged particles in the presence of an electric field. Electrokinetic effects may be controlled through suitable application of AC potentials or surface coating of the microfluidic channels.

The frequency dependence and dimension of the particle to be manipulated with DEP provides a large parameter space for tuning the dielectrophoretic properties of materials but also for analytical applications. This has also generated a substantial interest in the manipulation of proteins by DEP and its applications in protein separations despite the extremely large electric field gradients necessary to evoke large enough protein DEP [8,12]. Protein DEP has been typically reported as pDEP up to the MHz range [1,10,13–15] and some found a transition from pDEP to nDEP associated with a cross over frequency in the MHz range [1,13,15,16]. The experimental evidence of protein DEP has mainly been based on fluorescence observation at specific applied potential and frequency through changes in fluorescence intensities of labeled proteins [10,13–16].

Knowledge of the dielectric properties of proteins prior to DEP experiments would facilitate the design of protein DEP experiments as well as the applications in separation sciences. The prediction or determination of $Re[f_{CM}(\omega)]$ would thus be of great importance for future advances in protein DEP. Unfortunately, the current knowledge on protein polarization and its relation to DEP remains little explored. Additionally, the various experimental conditions and device characteristics under which protein DEP has been studied in the past impeded the development of a universal theory for protein DEP. However, established techniques such as electrochemical impedance spectroscopy (EIS) or dielectric spectroscopy (DS) could serve as a suitable pool of existing knowledge or if further developed provide valuable information on the polarization behavior of proteins under DEP conditions. EIS is a powerful tool for label-free analysis and characterization of biological systems such as cells, but also biomolecules such as DNA and proteins [17–19]. Impedance is inversely related to the complex permittivity of a sample [19]. Thus, $Re[f_{CM}(\omega)]$ can be quantified by EIS resultant from dielectric spectra [17,20]. Note that when EIS is used to study dielectric properties of materials, the technique is then called DS [19]. For several biological particles, the quantification of $Re[f_{CM}(\omega)]$ through EIS or DS has been performed, such as for example for various cell types [17,20–28]. The quantification of $Re[f_{CM}(\omega)]$ through EIS or DS has however not been explored in detail for proteins, as far as we know. However, a couple of publications have reported the use of EIS in combination with DEP for detection of proteins [29,30]. We suggest that EIS and DS could provide a useful knowledge pool for predicting the DEP behavior of proteins by quantifying the permittivity of proteins to determine the $Re[f_{CM}(\omega)]$ at a frequency of interest, as we will see in sections titled ‘Electrochemical impedance spectroscopy (EIS)’ and ‘Dielectric spectroscopy (DS) of proteins’.

In recent reviews [31,32], advances in purification, concentration and fractionation of proteins using DEP have been summarized; however, these review papers neither overview potential quantification methods to determine $Re[f_{CM}(\omega)]$ of proteins experimentally nor discuss the issues that have been preventing the quantification of protein polarizability which is the key to further DEP advances. In this review paper, we discuss EIS and DS as potential techniques to quantify the polarization of proteins via $Re[f_{CM}(\omega)]$ as well as the issues that have been the bottleneck for applying those techniques and suggest possible solutions. We start by summarizing the advances in protein DEP followed by the basis of EIS and its relation with DEP. Finally, we focused on the DS measurements of proteins, and its challenges for DEP applications including future perspectives. With the advent of microfabrication techniques and LOCs, it has been possible to perform EIS and DS experiments on biological particles suspended in physiological media [17,24,33–38], and we envision that those techniques will gain large importance in the determination of protein DEP behavior and the application of DEP for relevant biological techniques based on proteins.

Advances in protein DEP

DEP has proven to be a versatile mechanism for manipulating various micro- and nano-scale bioparticles (i.e., cells, viruses, bacteria, DNA and proteins) and has led to applications in separations [39–41] as well as diagnostics [42,43]. This potential of DEP for analytical purposes has also led to the interest for applications with proteins. In 2010, Garza-Garcia and Lapizco-Encinas [32] in their review paper reported only six research groups working with protein DEP, whereas by 2013 around 20 research groups were reported in a review by Nakano *et al*. [31] reflecting the great interests in protein DEP. In this section, we present a summary of the studies reporting protein DEP published after this review to date. Additionally, we will review the two most commonly employed techniques for protein DEP.

The microfluidic format is ideally suited as platform for protein DEP studies as it allows the generation of large electric fields and gradients thereof. Devices allowing manipulation of proteins by DEP have thus been integrated on LOCs in most cases. Their popularity is based on several key properties, such as high flexibility of design, low sample consumption, rapid analysis time and minimization of manual handling steps, which are of interest for bioanalytical applications. Devices like these therefore hold the promise of facilitating highly efficient, reproducible and standardized bioanalysis workflows coupled with low sample consumption. In addition, the integration in microfluidic devices renders laminar flow conditions for most applications and allows coupling of hydrodynamic and electrokinetic forces [8]. In particular, microfluidic devices for DEP applications seem highly suited to extend current protein separation methods as DEP has the potential to both serve as a concentration tool and as a separation tool.

Two major approaches have been implemented to create inhomogeneous electric fields for protein DEP: electrode-based DEP (eDEP) and insulator-based DEP devices (iDEP). eDEP devices can achieve inhomogeneous field gradients with low applied potentials by patterning microelectrodes integrated into microfluidic environments, see Figure 2A. However, eDEP involves disadvantages, such as electrode reactions occurring in the DEP manipulation

regions and field gradients localized around the microelectrodes [6–8]. iDEP devices emerged as an alternative device to overcome the common problems of eDEP devices. In iDEP devices, insulating obstacles are located inside of the channel while the electrodes are located at the inlet/outlet of the microfluidic device; see Figure 2B–D. The presence of the insulator structures distorts the electric field creating field gradients in a microfluidic channel. In iDEP devices homogeneous electric field gradients are established throughout the entire depth of the microfluidic channel [7, 8]. Nakano *et al*. [31] have recently reviewed the different devices reported for protein iDEP. Those iDEP devices for protein studies include nanoconstrictions [15], post-arrays [2,4], sawtooth [44] and nanostructures [9].

Since the first attempts of protein DEP, a wide variety of electrode- and insulator-based DEP microdevices have been developed, fabricated and successfully employed to manipulate and to separate bioparticles. Figure 2 provides a schematic of the most common DEP devices for protein DEP studies. Excellent reviews are available, summarizing realized geometries, devices and fabrication strategies [3,6–8,45] to which we refer the reader for more detail. The geometry of the microfluidic device is important since the literature indicates that protein DEP studies greatly depend on the design of the microfluidic device in addition to the other influences resulting from an interplay with electrokinetic effects (electroosmosis and electrophoresis) and diffusion properties of proteins.

Earlier literature focused on the realization of significant DEP forces acting on proteins and the advanced solutions generating large electric field gradients showed considerable promise. Large model proteins such as phycoerythrin [10] or well-characterized and stable proteins such as avidin or streptavidin [13] have been employed for demonstrations of protein DEP. In the last few years, the level of complexity has improved and the use of a larger variety of proteins with diagnostic importance has been reported. Liao *et al*. demonstrated a new method for protein enrichment in nanofluidic channels by nanoscale iDEP under physiological buffer conditions applying an AC signal [15,16]. Nakano *et al*. demonstrated a detailed investigation of factors influencing DEP of diagnostically relevant IgG molecules using an iDEP device under DC conditions [46]. A nanostructured insulator-based DEP approach was used to enhance enrichment of bovine serum albumin (BSA) by Camacho-Alanis *et al*. under DC conditions [9], and more recently for the study of the DEP behavior of β-galactosidase showing nDEP under DC and low-frequency conditions [11,47]. Staton *et al*. reported a novel method for concentration of Aβ amyloid fibrils [44]. Furthermore, the influence of device scaling in iDEP geometries for protein manipulation was investigated by Chaurey *et al*. [48]. Immobilization of proteins in a microelectrode and nanoelectrode array using DEP have also been reported recently by Hoelzel's group [49,50] and Sanghavi *et al*. [51] was able to preconcentrate neuropeptides for further electrochemical detection.

In all these examples, proteins are dissolved in buffer solutions for direct manipulation through DEP. However, novel strategies for protein DEP manipulation are emerging in recent years. For example, modified electrode surfaces with self-assembled monolayers of antibodies have been performed prior to protein manipulation in order to bind antigens [30]. A similar strategy has been reported using antibody-modified electrode surfaces to capture antigens with DEP [29,52]. An alternative strategy for protein DEP manipulation is the use

of colloidal particles or nanoparticles modified with proteins. Chuang *et al*. immobilized nanoparticles modified with antibodies using DEP, followed by binding antigens with previously immobilized antibodies [53]. A similar procedure was also reported for trapping BSA [54]. Honegger *et al*. modified Janus particles with fibronectin to later study the DEP behavior of those particles that have been selectively coupled with fibronectin [55]. Finally, Javanmard *et al*. [56] used a mixture of beads coated with IgG and demonstrated the removal of the protein from the buffer solution.

Although the experimental community has developed different approaches for protein DEP manipulation, as shown above, theoretical models as well as techniques predicting the DEP behavior of proteins should be further advanced to allow the experimentalists to improve existing approaches for applications. The theoretical models reported to predict the dielectrophoretic behavior are complex and a universal theory for protein DEP is not available [31]. Therefore, future frequency-dependent DEP studies on a large variety of proteins should allow developing refined theoretical models. On the other hand, several techniques have been proposed to predict $Re[f_{CM}(\omega)]$ including the particle motion method [57,58], optical tweezers [59,60], zeta potential measurements [61], electro-rotation [26] as well as EIS and DS measurements. In particular, EIS and DS have gained widespread use in developing biosensors [33], and have already been used to predict the DEP behavior of cells [22,26], and as a detection method for bacteria [62]. In addition, EIS has also been used to determine the DEP properties of DNA through measuring capacitance changes between microelectrodes [63]. However, EIS and DS have not yet been employed for the determination of the $Re[f_{CM}(\omega)]$ of proteins as far as we know.

The DEP behavior of several proteins as summarized in Table 1 has been mainly determined by localizing the area of protein concentration or trapping using fluorescence microscopy and was in some cases confirmed by numerical simulations. We can see from this table that most of the studies report pDEP behavior. Only the proteins BSA [4] and β-galactosidase [11,47] have been reported to demonstrate nDEP behavior under DC conditions while the nDEP behavior observed for Avidin was determined at high frequency [64]. However, the reported DEP behavior was in most cases not related to a quantitative analysis of $Re[f_{CM}(\omega)]$ or to theoretical models for the proteins listed in Table 1; only Clarke *et al*. [65,66] determined a particle conductivity of 24.6 S/m for yellow fluorescence protein showing pDEP under DC conditions, which can be used to calculate $Re[f_{CM}(\omega)]$ assuming only the conductivity of the protein and medium contribute to it.

DS and EIS measurements can potentially be used to determine the $Re[f_{CM}(\omega)]$ of proteins by determining the dielectric permittivity of the protein and the medium, as we will discuss below. In addition, the range of frequencies where the DS and EIS measurements can be performed is of great relevance since different information related to protein–protein and protein–water interactions can be obtained depending on frequency (see section titled ‘DS of proteins’). Moreover, according to mathematical approximations at low frequencies, the $Re[f_{CM}(\omega)]$ can be expressed in terms of only real conductivities of the particle and medium [71]. Hence, very low frequency measurements in EIS or DS could potentially be compared with DEP behavior under DC conditions.

On the other hand, DS and EIS measurements have to be detected in strategic regions (where the protein concentrates or gets trapped) because pH as well as temperature gradients can be generated along with microfluidic channels [72,73], and protein concentration varies along the channel which would influence the EIS/ DS measurements of the proteins under study [74,75]. In section titled 'Linking EIS and DS with DEP', we will discuss the integration of DS and EIS measurements in DEP devices suggesting existing microfluidic platforms that can be used for this purpose. Finally, EIS and DS techniques have the advantage of being label-free, which is of special interest in bioanalysis since it would eliminate the need to modify biomolecules with fluorescent dyes, enzymes, redox or radioactive labels [76]. Thus the integration of EIS and DS in an adequate DEP device could provide a useful tool in further understanding protein DEP without the need to label proteins.

Electrochemical impedance spectroscopy

The importance of electrochemical systems lies in the study of processes and factors that affect the transport of charge across the interface of an electrode in contact with an electrolyte solution. Two types of processes can occur in electrochemical systems: faradaic and non-faradaic processes. When electrochemical reactions are involved in the electrochemical cell, the process is called a faradaic process since such reactions are governed by Faraday's law [77]. However, processes such as diffusion, adsorption and desorption without the involvement of reactions are called non-faradaic processes [77]. The technique where the electrochemical cell or electrode impedance is measured and plotted versus frequency is termed EIS. EIS has been developed over the years to become a very strong experimental tool used in many fields investigating properties of semiconductors [78,79], in energy applications [80–83], corrosion [84,85] and biological systems [18,76,86] including the one discussed in this review.

Impedance is the ratio between voltage and current which has a real and imaginary term. The real impedance represents the ability of a circuit to resist the flow of electrical current, while the imaginary impedance term reflects the ability of a circuit to store electrical energy. In other words, impedance can be defined as a complex resistance encountered when current flows through a circuit composed of various resistors, capacitors and inductors. EIS is based on the measurement of the current flowing in the system under study as a consequence of a potential applied to the electrochemical system; see Figure 3A. The applied perturbation (AC signal) is usually a sinusoidal potential equal to $V = V_0 sin(\omega t)$ and, the emitted current response is equal to $I = I_0 sin(\omega t + \phi)$, where $\omega = 2\pi ft$ and f is the frequency. Hence, electrochemical impedance is defined as the complex number Z^* with the expression:

$$Z^* = \frac{V(t)}{I(t)} = \frac{V_0 \sin(\omega t)}{I_0 \sin(\omega t + \phi)} = |Z| \frac{\sin(\omega t)}{\sin(\omega t + \phi)} \quad \text{Equation 3}$$

Using Euler's relationship, $\exp(j(\varphi)) = \cos(\varphi) + j\sin(\varphi)$, Z^* can be expressed as a combination of real (Z_R) and imaginary (Z_{IM}) parts as follows:

$$Z^{*}=|Z|e^{j\phi}=|Z|\,(\cos\phi+j\sin\phi)=Z_{R}+jZ_{IM} \quad \text{Equation 4}$$

The phase angle at a chosen radial frequency is a ratio of the imaginary (Z_{IM}) and real (Z_R) impedance components:

$$\tan\phi=\frac{Z_{IM}}{Z_{R}} \quad \text{Equation 5}$$

EIS measurements are typically realized in a frequency range from mHz to MHz and usually represented in a Nyquist (Figure 3B) or Bode plot (Figure 3C). By varying experimental parameters such as applied current, temperature, reactant composition, etc. frequency shifts in the impedance spectra can be observed, revealing information on electrochemical processes (faradaic and/or non-faradaic) governing the system. However, the interpretation of impedance spectra can quickly become challenging, requiring the use of additional tools such as electrical equivalent circuit modeling [19], determination of relaxation times [87] or analysis of the difference in impedance spectra [88] for a better and deeper understanding.

The most common method to analyze impedance diagrams is using electrical equivalent circuits. This kind of analysis consists in fitting a measured impedance diagram with combination of ideal (resistor, capacitor, inductor, etc.) and non-ideal (constant phase element, Warburg element, etc.) electrical elements in series and/or in parallel [19]. Hence, the impedance diagram can be separated into different frequency ranges, each one represented by part of the equivalent circuit. This deconvolution of the impedance diagram allows distinguishing the main contributions governing the system considered. Equivalent circuits should always be selected on the basis of a detailed understanding of the electrochemical system, as long as it is based on the chemical and physical properties of the system and does not contain arbitrarily chosen circuit elements [19]. Since this method consists on fitting equivalent circuits with the experimental data, one has to be careful in choosing the correct equivalent circuit model. For instance, having an equivalent circuit that perfectly fits the experimental data does not necessarily mean that this equivalent circuit model has physical meaning. Therefore, one needs to apply knowledge of the physical processes involved, compare several equivalent circuit models with experimental data and attempt to simplify the representation as much as possible [19].

Determination of complex permittivity for DEP applications

The complex permittivity of biological material can be extracted from EIS measurements. Knowing the complex permittivity of the medium as well as the biological material of interest, the DEP behavior can be predicted as we will see in section titled ‘DS of Proteins’. Here, we review the equations that correlate the impedance with the complex permittivity ε^{*} as well as model theories such as the Maxwell–Wagner equation and its applications.

The dielectric analysis presents the permittivity and conductivity of a material as a combined complex permittivity formed by a real and imaginary component.

$$\varepsilon^*=\varepsilon' - j\varepsilon'' \quad \text{Equation 6}$$

The real permittivity component, ε′, is inversely related to Z_{IM} while the imaginary permittivity component represents the conductance of the material and is inversely proportional to Z_R [19], as shown in Equations 7 & 8:

$$\varepsilon'=\frac{k}{\omega}\left(\frac{1}{Z_{IM}}\right) \quad \text{Equation 7}$$

$$\varepsilon''=\frac{1}{Z_R}=\frac{\sigma}{\omega\varepsilon_0} \quad \text{Equation 8}$$

where *k* is the cell constant, σ the conductivity and ε_0 the vacuum permittivity. When dielectric properties are extracted by EIS, the method is typically called DS instead of EIS [19] However, DS uses the same type of electrical information as EIS but differs from its analysis and approach to data representation.

The impedance of a suspension depends on the sum of the current contributions through and around the suspended biological particle [19]. This allows to relate measured impedance with DEP properties. pDEP occurs when the permittivity of the particle is higher than the medium ($Z_p^*<Z_m^*$) aligning the dipoles with the field, causing attraction. In contrast, nDEP occurs when the permittivity of the particle is lower than the medium ($Z_p^*>Z_m^*$), then the induced dipole aligns against the field, causing repulsion of the particle [19]. Lvovich *et al*. [22] and in his book [19] defines the Re[$f_{CM}(\omega)$] factor in terms of impedance of the particle (Z_p^*) and the medium (Z_m^*) as:

$$Re[f_{CM}(\omega)]=\left(\frac{\varepsilon_p^*-\varepsilon_m^*}{\varepsilon_p^*+2\varepsilon_m^*}\right)=Re\left(\frac{Z_m^*-Z_p^*}{Z_m^*+2Z_p^*}\right) \quad \text{Equation 9}$$

However, we need to keep in mind that the total impedance is a mix of particles suspended in an electrolyte solution; hence, models have to be applied in order to determine Z_p^*. The Maxwell–Wagner model describes the impedance of a dilute suspension of particles. The model consists of defining the equivalent complex permittivity of the mixture in terms of the Re[$f_{CM}(\omega)$] and the ratio of the particle volume to the detection volume (volume fraction) defined by the following equation [26]:

$$\varepsilon_{mix}^*=\varepsilon_m^*\frac{1+2\delta f_{CM}}{1-\delta f_{CM}} \quad \text{Equation 10}$$

where ε_{mix}^* is the complex permittivity of the mixture and δ is the volume fraction.

Using the Maxwell–Wagner model in combination with EIS, Re[$f_{CM}(\omega)$] of bioparticles, specifically cells, has been reported in several publications [17,23–26]. However, because of

their complex and heterogeneous structure, cells cannot be considered as a simple sphere and are thus represented as single-shell or multi-shell particles depending on the specific cell type. In the single-shell model, the cell cytoplasm is considered as a conducting homogeneous sphere covered with a thin shell (cell membrane) [89]. In the multi-shell model, the spherical nucleus is also considered as a sphere having a thin shell, and the cytoplasm and cell membrane can be represented by another sphere with a thin shell forming a double shell [89]. Equivalent circuits are used to represent single-shell or multi-shell models to fit the impedance spectra allowing deriving dielectric properties for subcellular compartments.

For example, Sabunco *et al*. [24] used the Maxwell–Wagner model (Equation 10) to determine the $Re[f_{CM}(\omega)]$ of T-cell leukemia cells as well as an equivalent circuit to represent the double shell model, and fit the impedance spectra to determine the dielectric properties of cells such as the conductivity of the membrane, cytoplasm and nucleoplasm of the cell. Similarly, Valero *et al*. [17] determined the $Re[f_{CM}(\omega)]$ with the use of the Maxwell–Wagner equation for red blood cells and suggested an equivalent circuit to extract the dielectric properties of the cells. Other reports of determination of $Re[f_{CM}(\omega)]$ using the Maxwell–Wagner model in combination with EIS have also been reported for cell-derived microparticles [22], polystyrene beads [28] and tobacco mosaic virus [27]. In addition, Furst *et al*. determined the polarizability of beads (100 and 200 nm in size) using DS [20] by extrapolating data obtained with multiple spacer thickness to infinite separation [90–92] without directly using a Maxwell–Wagner model. Moreover, dielectric characterizations of nanoparticles (12–220 nm) with EIS have been reported in combination with Maxwell–Wagner theory [93] showing that the polarization mechanism is partially dependent on the surface charge and the size of the nanoparticles.

A basic understanding of the polarization of a suspended particle or colloids under an applied electric field can be explained as follows: when the electric field is applied to a colloid, the charged particle and its electric double layer (EDL) will be forced into motion, with particle and counterions moving in opposite direction [93]. Migration and convection of ions induce an ionic current along the particle surface which polarizes the EDL and changes the dipole moment. At the same time, the electrophoretic migration of the particle in response to the applied electric field also polarizes the EDL and modifies the strength of the dipole moment [94]. A classical model to describe the dielectric properties of particles is the Maxwell–Wagner model valid at high frequencies [28,94–96] since the influence of the bulk solution on the dipole moment of the particle at low frequencies is not accounted for in this model. The Dukhin–Shilov theory extends to low frequencies [94,97,98]; however, both Maxwell–Wagner and Dukhin– Shilov theories are restricted to thin EDL (compared with the particle radius) and do not consider the influence of electrophoresis on the dipole moment [94]. A more detailed model compared with Maxwell–Wagner or Dukhin–Shilov model is the Poisson–Nernst– Planck equation (PNP) taking into account migration, convection and diffusion of ions as well as the particle's electrophoretic migration [94,95]. In addition, the PNP model is not restricted to thick EDLs, for instance, the PNP model has been applied for nanoscale particles surrounded by a thick EDL [99,100]. Zhao and Bao [100] used this model to study nanorods reporting the effect of size on the dipole moment

showing a good agreement with experimental data for short DNA molecules. According to their results [100], the finite ion mobility prevents the ions from responding to the applied electric field at high frequencies. When the frequency decreases, ions in the EDL have sufficient time to migrate along the particle surface and accumulate at the ends of the rod, polarizing the EDL [100]. Since the distance between the separated charges (accumulating at the ends of the rod) increases as the length of the rod increases, the magnitude of the dipole moment also increases [94,100]. The PNP model has also been used to calculate the dipole moment of spherical nanoparticles [101,102], and two dimensional cylindrical particles with the electric field transverse to their axis [95]. Although proteins have more complicated structure than nanoparticles or nanorods, these considerations might also apply for proteins and could improve the understanding of the protein polarization mechanism at high and low frequencies.

With the appropriate model, the polarizability of proteins can be determined depending on the frequency range. At high frequency, the dipole moment can be potentially determined in combination of Maxwell–Wagner theory with EIS measurements. At low frequencies, diffusion and electrokinetic effects (Dukhin–Shilov or PNP theory) have to be considered besides the contributions of the Maxwell–Wagner model to determine the permittivity with EIS. These current models might, however, be refined and adapted to specific proteins. Additionally, electrode polarization (EP) effects occur at low frequency creating noise and complicating the EIS measurements. This effect will be described in more detail in the section of Electrode Polarization Effects with possible solutions. As far as we know, EIS has not yet been directly used to determine the $Re[f_{CM}(\omega)]$ of proteins. However, estimations can be performed from previous DS studies of proteins as we will show in the next chapter. Nevertheless, EIS is a promising technique to study the DEP behavior of proteins, and we encourage the experimental community to incorporate this technique in their research for protein DEP.

DS of proteins

The dielectric properties of biological systems typically display extremely high dielectric permittivity at low frequencies, decreasing in more or less distinct steps with increasing frequency, as shown in Figure 4. Their frequency dependence permits identification and investigation of a number of different underlying mechanisms. DS is especially sensitive to interface polarization and intermolecular (dipole–dipole) interactions, and cooperative processes may be monitored [103]. DS is correlated to EIS through the relations of impedance to permittivity as can be seen from Equations 7 & 8; however, DS differs from EIS due to its analysis and approach to data representation. One of the main interests of performing DS measurements is to determine the dielectric relaxation of molecules, which is a measure of the time scale for reorientation of the molecule [19,104]. The concept of dielectric relaxation was first introduced by Maxwell and Debye, who used it to describe the time (τ) required for dipolar molecules to reversely orient themselves in the external AC electric field. The time required for that process to take place was called relaxation time and it is inversely related to the critical relaxation frequency (fc) with $\tau = \frac{1}{2}\pi f_C$ [19]. DS measures relaxation times by plotting the complex permittivity ε^* versus the frequency.

Protein solutions have dielectric relaxation due to orientation of polar molecules and counterion fluctuations [105]. Dielectric spectra of aqueous protein solutions generally extend over a broad frequency range, from a few kHz to tens of GHz consisting of different and partially overlapping regions originating from different polarization mechanisms at the molecular level [106]. In a dielectric spectrum of a protein solution, a fairly large relaxation is observed in the range of approximately 0.1–1 MHz called β-dispersion corresponding to the orientational relaxation of protein dipoles [107]. The δ-dispersion, located in between β- and γ-dispersion (see Figure 4), is still a subject of discussion [108]. First indications for δ-dispersions where found by Haggis and Buchanan [109,110]. δ-Dispersion is considered to include the orientational relaxation of dipoles of water molecules in the hydration shell, flexible loops or side chains of proteins [111]. It is generally accepted nowadays that this dispersion is due to bound water relaxation; however, the complexity of proteins makes it difficult to decide if the δ-dispersion can solely be explained by a bound water relaxation or if additional effects like intra-protein motions have to be included [108]. In the microwave frequency range, large relaxation with an absorption peak at ∼20 GHz is termed g-dispersion corresponding to the orientational relaxation of bulk water dipoles [112]. Finally, α-dispersions are generally associated with the diffusion processes of ionic species in the low frequency range (1–100Hz) and are governed by the solvent dynamics [35,108]. Figure 4 shows a schematic view of the four dispersions located at their particular frequency range.

As we mentioned before, the polarization of proteins depends on the protein structure, type of buffer (e.g., conductivity and pH) and protein concentration. Oleinikova *et al*. [74] demonstrated that the dipole moment of proteins decreases with the concentration due to protein–protein interactions. For globular proteins, the reorientation is a process controlled by the hydrodynamic friction of the solvent [113]. Therefore, the polarization of proteins not only depends on the reorientation of the polar side groups, vibrations of the polypeptide backbone and fluctuating proton transfer between ionized side groups of the protein, but also on the torque exerted on each water dipole moment to align along the direction of the field vector [74,75,113]. In conclusion, the polarization of proteins is a more complex process as compared with nanoparticles and the available models describing nanoparticle polarization might need further refinement to fully describe protein polarization.

Although dielectric properties of proteins using DS have been studied intensively [103,114-116], the determination of $Re[f_{CM}(\omega)]$ of proteins through DS is not usually reported. However, having determined the permittivity of the protein and the medium, the $Re[f_{CM}(\omega)]$ can be deducted. As an example, the $Re[f_{CM}(\omega)]$ for myoglobin and lysozyme can be calculated with Equation 1 with permittivities as previously obtained with DS measurements. Figure 5 shows the $Re[f_{CM}(\omega)]$ values for myoglobin and lysozyme calculated from references [117] and [106], respectively. The dielectric data of water were obtained from reference [118].

From Figure 5, we can see that nDEP of lysozyme is expected at high frequencies from 10 MHz to 10 GHz, which agrees with DEP behavior modeled in Matyushov's report [119]. In the case of myoglobin, a change of the DEP behavior is expected from nDEP to pDEP in the high frequency range between 10 MHz and 10 GHz. This can be compared with a model developed by Gunda *et al*. [120]. In their simulations, a dielectric myoglobin model is

developed by approximating the shape of the myoglobin molecule as sphere, oblate and prolate spheroid. According to this model, the crossover frequency for myoglobin from nDEP to pDEP is expected at 40 MHz [120], which is a lower frequency compared with our estimations of the $Re[f_{CM}(\omega)]$ for myoglobin, see Figure 5. This discrepancy of this report in comparison with our calculations might be due to variations in the experimental conditions reported in the literature from which we extracted the underlying information for Figure 5.

Nevertheless, this comparison demonstrates that one could expect significant differences in the magnitude of DEP forces leading to different DEP-based migration. In the frequency range in which the two proteins show nDEP, they should be distinguished with their different DEP migration due to a differing magnitude of the Clausius–Mossotti factor. This points toward a possible separation mechanism despite the similar size of the proteins: ∼15 kDa for lysozyme versus ∼17 kDa for myoglobin. Moreover, at larger frequencies, the coexistence of nDEP and pDEP would even indicate a stronger difference in their DEP behavior. For example, we speculate that the two proteins could be separated by a streaming DEP application, fractionating the two proteins into different streams on a microfluidic platform. Similar approaches have been developed with other biological species [40,121–124].

It is important to mention that one difficulty to calculate the $Re[f_{CM}(\omega)]$ of proteins from previous studies is to find the dielectric spectra of the medium under the same conditions as the DS measurements were carried out for the particular protein of interest. Nevertheless, these calculations show the importance of DS measurements to predict the DEP behavior of proteins. Moreover, DS studies with proteins are usually performed at very high frequencies (>MHz) to avoid EP effects. Extrapolation to lower frequencies, such as for example used in iDEP applications becomes difficult. Some reports however included DS at low frequencies by careful experimental approaches such as the recent publications of Roy *et al*. [125], Jansson *et al*. [126] and Kyritsis *et al*. [127]. Limitations of protein DS include sensitivity of the measuring apparatus and polarization due to the double layer that forms at the electrode/solution interface (EP) [128] which will be discussed next.

EP effects

A main factor affecting the accuracy of DS measurements is EP. When EP occurs, the dielectric spectra of the protein of interest are greatly influenced by the signal of EP at low frequencies (<1 kHz). Therefore, DS measurements of proteins at low frequencies are a challenge. EP occurs when ions migrate toward the electrode or sample interface under the influence of an electric field, leading to the development of ionic double layers in these regions producing a strong voltage drop. The resultant capacitance of these double layers can dominate the signal at lower frequencies (<1 kHz), masking the dielectric properties of the system under study. Several correction techniques have been developed to minimize EP effects which include the following.

Algorithm corrections

Algorithm corrections include mathematical models that define functions that correlate the capacitance due to the EP [129,130]. Therefore, knowing the EP capacitance through algorithms, the impedance of experimental data can be corrected by subtraction.

Comparison & substitution methods

In this method the evaluation of the EP is based on an additional measurement of a reference material with well-defined dielectric parameters and having the same conductivity as the sample. For example, Valero *et al*. [17] used this approach to determine $\mathrm{Re}[f_{CM}(\omega)]$ of red blood cells by quantifying the impedance difference of the microfluidic channel with and without cells. Thus, elimination of EP could be implemented by subtraction of the reference spectrum from the spectrum of the probe; however, this approach is only successful if the conductivity of the medium in both experiments is the same.

Electrode-coating techniques

The overall idea is to maximize the electrode–electrolyte interface area which is inversely proportional to the EP impedance by increasing the surface area. In other words, high surface area (rougher/porous electrodes) and highly conductive electrode materials will reduce EP [129]. This can be achieved either by mechanical or electrochemical treatments that produce porous or fractal metal interfaces with a large effective surface area [131] or by selecting electrodes such as conductive polymers [132] and carbon electrodes [133,134] which are porous and therefore have higher surface area. Carbon electrodes have already been used in DEP applications [8,135] and their use could be advantageous for DS measurements of proteins.

Hardware-based techniques

The design of the electrodes as well as the complete electrochemical cell has an important impact on EP effects. To this respect, it is of importance to use electrodes as small as possible to improve sensitivity [33,131]. Micro- and nanofabrication is an excellent tool that can make this possible. Current DEP devices can potentially be used in combination with EIS and DS. As mentioned before, two main types of DEP devices are used: eDEP and iDEP. However, if EIS and DS measurements are incorporated, additional electrodes have to be integrated (e.g., working electrode and counter electrode) in the regions where the protein is concentrated or trapped. Those electrodes are connected to a potentiostat and might be different from those inducing the electric field gradient.

Another DEP microfluidic design that has not been used yet for EIS and DS measurements combined with DEP but can potentially be used is contactless DEP (cDEP), see Figure 6A. cDEP is an extension of iDEP where the electrodes are located outside the microfluidic channel avoiding direct contact with the electrolyte solution [136,137] potentially eliminating EP effects to a large extent. Electrodes not connected to the microfluidic channel as realized in cDEP devices can be connected to the potentiostat for EIS and DS measurements, while electrodes in the inlet/outlet of the microfluidic channel induce the electric field gradient at insulating constrictions. In addition, Davalos *et al*. [138] patented

an iDEP device with integrated electrodes for impedance measurements of cells where electrodes for EIS measurements were located on the side of the microfluidic walls, see Figure 6B. In this case, cells were concentrated through iDEP while EIS could be performed at the same time (real-time measurements) [138].

Devices such as cDEP or iDEP typically require higher applied potentials than eDEP devices. An alternative strategy involves the use of carbon-DEP devices and their application similar to the schematic shown in Figure 6C. Carbon-DEP combines some of the advantages of metal-based eDEP and iDEP, where electrodes are made by carbonizing a patterned photoresist [135] rendering a conductive carbon material that can be used as an electrode. Therefore, we can potentially design carbon-DEP devices with additional electrodes for DS and EIS measurements. Hardware-based techniques can be combined with the algorithm corrections, substitution methods and electrode coating techniques mentioned above to reduce or eliminate EP for protein EIS and DS studies at low frequency. In addition, the resolution of low frequency modes can also be improved by electrical cleaning as found in a recent publication by Richert's group [125]. Finally, modifying electrodes with bio-films or self-assembled monolayers is another strategy to reduce EP effects by forming a layer protecting the electrode from EP effects [30,51,53,54,139,140].

Another important aspect of EP is its dependence on solution conductivity and temperature. Mazzeo and Flewitt [141] discussed in their paper that the phase angle measured by impedance analyzer instruments is intrinsically dependent on the conductivity of the solution. In general, phase angle resolution constraints due to high conductivity solutions prohibit many experiments in high salt concentrations [141]. This is one reason that most DS experiments are performed in solutions with an ionic strength less than 1 mM [142]. Ions affect the conductivity according to their individual ionic mobilities, thus, different buffer ions will result in different conductivities at equal concentrations. Hence, one important step to perform DS measurements is selecting an appropriate impedance analyzer following the arguments by Mazzeo and Flewitt [141] as well as an appropriate buffer system. In addition, there are several approaches of EP correction that have been proposed for DS measurements in high conductivity media. All of them are based on the different model descriptions of the EP process, experimental estimation of its magnitude and subtraction of the EP component from the raw signal in the frequency or time domain [103]. In addition, the electrical double layer also depends critically upon the chemical nature of the sample being investigated as well as upon the chemical and physical nature of the electrodes used [103]; therefore, a suitable microfluidic design and electrode material can also be applied to improve DS measurements at high conductivity. It is interesting to note that the DEP device used by Liao *et al*. [15] has been capable to concentrate proteins in physiological media. In addition, Krishnan *et al*. [143,144] have performed DEP studies of DNA and nanoparticles in high conductivity media using a microarray device with hydrogel over-coated microelectrodes. Such approaches could potentially be applied to DS measurements. Finally, using a four electrode instead of the typically employed two electrode configuration as suggested by Mazzeo *et al*. [141] could further reduce EP effects.

Finally, the conductivity dependence on temperature – usually described by the Arrhenius equation [19] – is important since Joule heating effects can occur in DEP experiments

[48,145]. This is especially important in the case where EIS and DS measurements are incorporated in iDEP devices since iDEP devices require higher applied potentials to overcome electrokinetic effects resulting in Joule heating effects. Nakano *et al*. [73] determined that the temperature in iDEP devices fluctuates from room temperature to 34°C at 3000 V/cm with a conductivity of 300 μS/cm. However, smaller applied electric fields did not show appreciable temperature increases. We should thus expect higher temperature fluctuations with higher medium conductivity. Fortunately, the temperature dependence of the dielectric properties of proteins is stronger at low temperatures (<293 K) than at higher temperature [115]; this implies that the dielectric spectra of proteins might not be influenced through Joule heating effects if DEP concentration would be used in dielectric measurements.

As we have demonstrated with this section, EP presents an important challenge faced in performing DS measurements at low frequencies. However, understanding and suppressing EP in DS applications could also be viewed as an opportunity in itself considering the importance of the interface and the several options to correct and to minimize EP effects.

Linking EIS & DS with DEP

In order to incorporate EIS and DS measurements in DEP devices, the first step is to engineer DEP devices that incorporate electrodes for EIS and DS measurements. One way is to incorporate interdigitated microelectrodes in the microfluidic channel presenting promising advantages in terms in low ohmic drop and fast establishment of the steady state [33]. Most of the EIS measurements for DEP applications have utilized eDEP devices [17,26,146]. Those studies have been mainly focused on label free detection of biomolecules which is very attractive in the field. However, patterning electrodes in microfluidic devices (eDEP) has the disadvantage of not covering the complete height of the microfluidic channel which might result in missing information during the EIS and DS measurements. Martinez-Duarte *et al*. [147] have developed interdigitated microelectrodes made of carbonized photoresist (carbon electrodes) with the unique characteristic that those interdigitated carbon electrodes can be easily patterned with flexible shapes covering the entire depth of the channel (3D carbon-DEP device) [8], see Figure 6C. This type of interdigitated device can potentially be used in the future for EIS and DS measurements. An alternative device that can also be used for EIS and DS measurements is cDEP [136] as mentioned in the previous section, see Figure 6B.

Finally, another novel approach to incorporate EIS and DS measurements is using liquid electrodes in an iDEP device such as developed by Demierre and coworkers [148,149]. This novel device is based on the use of planar electrodes fabricated on the bottom of dead-end chambers placed on the side of the main flowing channel. For instance, a non-invasive, label-free method has recently been developed for morphology-based cell sensing based on EIS measurements using this kind of device [36]. In addition, a recent protein DEP work used an iDEP device to preconcentrate proteins through nDEP where carbon electrodes were located at the nDEP regions adsorbing proteins. After preconcentration with the iDEP device, the carbon electrodes with adsorbed proteins were connected to perform electrochemical studies [51]. Moreover, Davalos *et al*. have already proposed an iDEP

device integrating electrodes for sensing cells via EIS measurements, see Figure 6A. Those are examples of the variety of microfluidic devices that can potentially be designed to integrate iDEP devices with EIS measurements.

Conclusion

We have reviewed the experimental approaches and potential of EIS and DS measurements to reveal useful information for DEP experiments of proteins. EIS is a technique that elucidates dielectric properties to identify and characterize biomolecules such as proteins. The main difference between EIS and DS is the data analysis and approach for data representation. There is also extended information available on DS of proteins; however, this knowledge has not been directly used to determine $Re[f_{CM}(\omega)]$ which would help to understand the DEP behavior of proteins. We thus provided an estimation of the $Re[f_{CM}(\omega)]$ of lysozyme and myoglobin adapted from previous reports as an example. This demonstrates that the DEP properties of proteins could be obtained in a variety of frequency ranges and useful design parameters for bioanlaytical applications may be extracted. In addition, we have discussed remaining challenges in EIS and DS and gave alternatives to reduce the EP effects. With this knowledge we propose that DEP devices with incorporated EIS and DS capabilities could make an impact to elucidate protein DEP but also provide improved methodology for protein manipulation by DEP.

Future perspective

Since the number of research groups that have studied protein DEP have been increased more than three-times from 2010 to 2013, we expect this method to be of importance for bioanalytical applications. Knowing the dielectrophoretic properties of proteins is imperative to create strategies for their future separation and purification by DEP. The link between dielectric properties obtained from methods such as EIS and DS is important to improve the field and deduct predictions for the parameters suitable for protein DEP. With adequate selection of literature data, this is already possible and promising as shown in this review.

Furthermore, the direct coupling of EIS or DS capabilities in DEP devices has the advantage to extract dielectric properties under the same experimental conditions. Moreover, the impedance readout has the advantage of not requiring protein labeling thus allowing for the study of native proteins. However, the combined approach requires several experimental challenges to be overcome, such as EP and the adequate theoretical model. With the refinement of device designs, microfluidic integration and appropriate nanotechnological approaches, these challenges might be addressed successfully for proteins. We expect important information to be gained through the incorporation of DS and EIS measurements in devices also suitable for protein DEP. Finally, a large variety of proteins need to be investigated in the future to truly elucidate the analytical applications in which protein DEP will play a role.

Acknowledgments

The authors acknowledge financial support by the National Center for Research Resources (5R21RR025826-03) and the National Institute of General Medical Sciences (8R21GM103522-03) from the National Institutes of Health.

References

Papers of special note have been highlighted as:

• of interest; •• of considerable interest.

1. Hughes, MP. Nanoelectromechanics in Engineering and Biology. CRC Press; USA: 2003. p. 37-38.
2. Nakano A, Chao TC, Camacho-Alanis F, Ros A. Immunoglobulin G and bovine serum albumin streaming dielectrophoresis in a microfluidic device. Electrophoresis. 2011; 32:2314–2322. [PubMed: 21792990]
3. Lapizco-Encinas BH, Rito-Palomares M. Dielectrophoresis for the manipulation of nanobioparticles. Electrophoresis. 2007; 28:4521–4538. [PubMed: 18072220]
4. Lapizco-Encinas BH, Ozuna-Chacon S, Rito-Palomares M. Protein manipulation with insulator-based dielectrophoresis and direct current electric fields. J Chromatogr A. 2008; 1206:45–51. [PubMed: 18571183]
5. Chao TC, Hansmeier N. Microfluidic devices for high-throughput proteome analyses. Proteomics. 2013; 13:467–479. [PubMed: 23135952]
6. Khoshmanesh K, Nahavandi S, Baratchi S, Mitchell A, Kalantar-zadeh K. Dielectrophoretic platforms for bio-microfluidic systems. Bios Bioelectron. 2011; 26:1800–1814.
7•. Li M, Li WH, Zhang J, Alici G, Wen W. A review of microfabrication techniques and dielectrophoretic microdevices for particle manipulation and separation. J Phys D: Appl Phys. 2014; 47:1–29. Review paper related to microfabrication of dielectrophoresis (DEP) devices.
8•. Martinez-Duarte R. Microfabrication technologies in dielectrophoresis applications-A review. Electrophoresis. 2012; 33:3110–3132. Review paper related to microfabrication of DEP devices. [PubMed: 22941778]
9. Camacho-Alanis F, Gan L, Ros A. Transitioning streaming to trapping in DC insulator-based dielectrophoresis for biomolecules. Sens Actuators B Chem. 2012; 173:668–675. [PubMed: 23441049]
10. Holzel R, Calander N, Chiragwandi Z, Willander M, Bier FF. Trapping single molecules by dielectrophoresis. Phys Rev Lett. 2005; 95:128102-1–128102-4. [PubMed: 16197115]
11. Nakano, F.; Camacho-Alanis, F.; Ros, A. Insulator- based dielectrophoretic behavior of β-galactosidase under DC and low frequency AC conditions. Presented at: 18th μTAS Proceedings; San Antonio, Texas, USA. 2014. 978–970–9798064–7–6
12. LaLonde A, Gencoglu A, Romero-Creel MF, Koppula KS, Lapizco-Encinas BH. Effect of insulating posts geometry on particle manipulation in insulator based dielectrophoretic devices. J Chromatogr A. 2014; 1344:99–108. [PubMed: 24767832]
13. Bakewell DJG, Hughes MP, Milner JJ, Morgan H. Dielectrophoretic manipulation of avidin and DNA. Ann Int IEEE Embs. 1998; 2:1079–1082.
14. Zheng LF, Brody JP, Burke PJ. Electronic manipulation of DNA, proteins, and nanoparticles for potential circuit assembly. Biosens Bioelectron. 2004; 20:606–619. [PubMed: 15494246]
15. Liao KT, Tsegaye M, Chaurey V, Chou CF, Swami NS. Nano-constriction device for rapid protein preconcentration in physiological media through a balance of electrokinetic forces. Electrophoresis. 2012; 33:1958–1966. [PubMed: 22806460]
16. Liao KT, Chou CF. Nanoscale molecular traps and dams for ultrafast protein enrichment in high-conductivity buffers. J Am Chem Soc. 2012; 134:8742–8745. [PubMed: 22594700]
17. Valero A, Braschler T, Renaud P. A unified approach to dielectric single cell analysis: Impedance and dielectrophoretic force spectroscopy. Lab Chip. 2010; 10:2216–2225. [PubMed: 20664865]
18. Randviir EP, Banks CE. Electrochemical impedance spectroscopy: an overview of bioanalytical applications. Anal Methods. 2013; 5:1098–1115.

19•. Lvovich, VF. Impedance Spectroscopy: Applications to Electrochemical and Dielectric Phenomena. J. Wiley & Sons; Hoboken, New Jersey, USA: 2012. Recommended book for electrochemical impedance spectroscopy (EIS) and dielectric spectroscopy (DS). This book also covers a DEP section

20. Beltramo PJ, Furst EM. Predicting the disorderorder transition of dielectrophoretic colloidal assembly with dielectric spectroscopy. Electrophoresis. 2013; 34:1000–1007. [PubMed: 23203650]

21. Gagnon Z, Gordon J, Sengupta S, Chang HC. Bovine red blood cell starvation age discrimination through a glutaraldehyde-amplified dielectrophoretic approach with buffer selection and membrane cross-linking. Electrophoresis. 2008; 29:2272–2279. [PubMed: 18548460]

22. Lvovich V, Srikanthan S, Silverstein RL. A novel broadband impedance method for detection of cell-derived microparticles. Biosens Bioelectron. 2010; 26:444–451. [PubMed: 20729061]

23. Sabuncu AC, Beskok A. A separability parameter for dielectrophoretic cell separation. Electrophoresis. 2013; 34:1051–1058. [PubMed: 23348751]

24. Sabuncu AC, Zhuang J, Kolb JF, Beskok A. Microfluidic impedance spectroscopy as a tool for quantitative biology and biotechnology. Biomicrofluidics. 2012; 6:034103-1–034103-15.

25. Sun T, Gawad S, Green NG, Morgan H. Dielectric spectroscopy of single cells: time domain analysis using Maxwell's mixture equation. J Phys D: Appl Phys. 2007; 40:1–8.

26. Morgan H, Sun T, Holmes D, Gawad S, Green NG. Single cell dielectric spectroscopy. J Phys D: Appl Phys. 2007; 40:61–70.

27. Ermolina I, Morgan H, Green NG, Milner JJ, Feldman Y. Dielectric spectroscopy of Tobacco Mosaic Virus. Biochim Biophys Acta. 2003; 1622:57–63. [PubMed: 12829262]

28. Green NG, Morgan H. Dielectrophoresis of submicrometer latex spheres. 1. Experimental results. J Phys Chem B. 1999; 103:41–50.

29. Li S, Cui H, Yuan Q, et al. AC electrokinetics-enhanced capacitive immunosensor for point-of-care serodiagnosis of infectious diseases. Biosens Bioelectron. 2014; 51:437–443. [PubMed: 24007749]

30. Cheng IF, Yang HL, Chung CC, Chang HC. A rapid electrochemical biosensor based on an AC electrokinetics enhanced immuno-reaction. Analyst. 2013; 138:4656–4662. [PubMed: 23776933]

31•. Nakano A, Ros A. Protein dielectrophoresis: advances, challenges, and applications. Electrophoresis. 2013; 34:1085–1096. Review paper related to protein DEP. [PubMed: 23400789]

32. Garza-Garcia LD, Lapizco-Encinas BH. State of the art on protein manipulation employing dielectrophoresis. Rev Mex Ingeniería Química. 2010; 9:125–137.

33. Varshney M, Li Y. Interdigitated array microelectrodes based impedance biosensors for detection of bacterial cells. Biosens Bioelectron. 2009; 24:2951–2960. [PubMed: 19041235]

34. Cheung K, Gawad S, Renaud P. Impedance spectroscopy flow cytometry: on-chip label-free cell differentiation. Cytometry A. 2005; 65A:124–132. [PubMed: 15825181]

35. Heileman K, Daoud J, Tabrizian M. Dielectric spectroscopy as a viable biosensing tool for cell and tissue characterization and analysis. Biosens Bioelectron. 2013; 49:348–359. [PubMed: 23796534]

36. Shaker M, Colella L, Caselli F, Bisegna P, Renaud P. An impedance-based flow microcytometer for single cell morphology discrimination. Lab Chip. 2014; 14:2548–2555. [PubMed: 24874178]

37. Mernier G, Duqi E, Renaud P. Characterization of a novel impedance cytometer design and its integration with lateral focusing by dielectrophoresis. Lab Chip. 2012; 12:4344–4349. [PubMed: 22899298]

38. Kuettel C, Nascimento E, Demierre N, et al. Label-free detection of Babesia bovis infected red blood cells using impedance spectroscopy on a microfabricated flow cytometer. Acta Trop. 2007; 102:63–68. [PubMed: 17451631]

39. Luo J, Abdallah BG, Wolken GG, Arriaga EA, Ros A. Insulator-based dielectrophoresis of mitochondria. Biomicrofluidics. 2014; 8(2):021801-1–021801-11. [PubMed: 24959306]

40. Jaramillo MC, Torrents E, Martinez-Duarte R, Madou MJ, Juarez A. On-line separation of bacterial cells by carbon-electrode dielectrophoresis. Electrophoresis. 2010; 31:2921–2928. [PubMed: 20690146]

41. Abdallah BG, Chao TC, Kupitz C, Fromme P, Ros A. Dielectrophoretic sorting of membrane protein nanocrystals. ACS Nano. 2013; 7:9129–9137. [PubMed: 24004002]
42. Braff WA, Willner D, Hugenholtz P, Rabaey K, Buie CR. Dielectrophoresis-based discrimination of bacteria at the strain level based on their surface properties. PLoS ONE. 2013; 8(10):e76751. [PubMed: 24146923]
43. Demircan Y, Ozgur E, Kulah H. Dielectrophoresis: applications and future outlook in point of care. Electrophoresis. 2013; 34:1008–1027. [PubMed: 23348714]
44. Staton SJR, Jones PV, Ku G, et al. Manipulation and capture of A beta amyloid fibrils and monomers by DC insulator gradient dielectrophoresis (DC-iGDEP). Analyst. 2012; 137:3227–3229. [PubMed: 22575916]
45. Srivastava SK, Gencoglu A, Minerick AR. DC insulator dielectrophoretic applications in microdevice technology: a review. Anal Bioanal Chem. 2011; 399:301–321. [PubMed: 20967429]
46. Nakano A, Camacho-Alanis F, Chao TC, Ros A. Tuning direct current streaming dielectrophoresis of proteins. Biomicrofluidics. 2012; 6 034108-1-04108-13.
47. Nakano A, Camacho-Alanis F, Ros A. Insulator-based dielectrophoresis with β-galactosidase in nanostructured devices. Analyst. 2014; 140:860–868. [PubMed: 25479537]
48. Chaurey V, Rohani A, Su YH, et al. Scaling down constriction-based (electrodeless) dielectrophoresis devices for trapping nanoscale bioparticles in physiological media of high-conductivity. Electrophoresis. 2013; 34:1097–1104. [PubMed: 23436401]
49. Otto S, Kaletta U, Bier FF, Wenger C, Hoelzel R. Dielectrophoretic immobilisation of antibodies on microelectrode arrays. Lab Chip. 2014; 14:998–1004. [PubMed: 24441950]
50. Laux EM, Kaletta UC, Bier FF, Wenger C, Hoelzel R. Functionality of dielectrophoretically immobilized enzyme molecules. Electrophoresis. 2014; 35:459–466. [PubMed: 24254805]
51•. Sanghavi BJ, Varhue W, Chavez JL, Chou CF, Swami NS. Electrokinetic preconcentration and detection of neuropeptides at patterned graphene-modified electrodes in a nanochannel. Anal Chem. 2014; 86:4120–4125. Publication incorporating electrodes at negative dielectrophoresis (nDEP) regions to trap peptides for further electrochemical detection. [PubMed: 24697740]
52. Laio, KT.; Swami, SN.; Chou, CF. Rapid monitoring low abundance prostate specific antigen by protein nanoconstriction molecular dam. Presented at: The 17th International Conference on Miniaturized Systems for Chemistry and Life Sciences; Frelburg, Germany. 27–31 October 2013; p. 1406-1408.
53. Chuang CH, Wu HP, Huang YW, Chen CH. Enhancing of intensity of fluorescence by DEP manipulations of polyaniline-coated Al2O3 nanoparticles for immunosensing. Biosens Bioelectron. 2013; 48:158–164. [PubMed: 23680934]
54. Chuang CH, Ju JW, Huang YW. Enhancing fluorescent response of immunosensing by a dielectrophoresis chip with transparent electrodes and microcavities array. Micro Nano Lett. 2013; 8:659–663.
55. Honegger T, Peyrade D. Dielectrophoretic properties of engineered protein patterned colloidal particles. Biomicrofluidics. 2012; 6:044115-1–044115-12.
56. Javanmard M, Emaminejad S, Gupta C, et al. Depletion of cells and abundant proteins from biological samples by enhanced dielectrophoresis. Sens Actuators B Chem. 2014; 193:918–924.
57. Pethig R, Bressler V, Carswell-Crumpton C, et al. Dielectrophoretic studies of the activation of human T lymphocytes using a newly developed cell profiling system. Electrophoresis. 2002; 23:2057–2063. [PubMed: 12210259]
58. Pethig R, Talary MS. Dielectrophoretic detection of membrane morphology changes in Jurkat T-cells undergoing etoposide-induced apoptosis. IET Nanobiotechnol. 2007; 1:2–9. [PubMed: 17500582]
59. Wei MT, Junio J, Ou-Yang HD. Direct measurements of the frequency-dependent dielectrophoresis force. Biomicrofluidics. 2009; 3:012003-1–012003-8.
60. Hong Y, Pyo JW, Baek SH, et al. Quantitative measurements of absolute dielectrophoretic forces using optical tweezers. Opt Lett. 2010; 35:2493–2495. [PubMed: 20634874]
61. Basuray S, Chang HC. Designing a sensitive and quantifiable nanocolloid assay with dielectrophoretic crossover frequencies. Biomicrofluidics. 2010; 4:013205-1–013205-11.

62. Hamada R, Takayama H, Shonishi Y, et al. A rapid bacteria detection technique utilizing impedance measurement combined with positive and negative dielectrophoresis. Sens Actuators B Chem. 2013; 181:439–445.
63. Henning A, Bier FF, Hoelzel R. Dielectrophoresis of DNA: quantification by impedance measurements. Biomicrofluidics. 2010; 4:022803-1–022803-9. [PubMed: 20697597]
64. Washizu M, Suzuki S, Kurosawa O, Nishizaka T, Shinohara T. Molecular dielectrophoreisis of biopolymers. IEEE Trans Ind Appl. 1994; 30:835–843.
65. Clarke RW, White SS, Zhou DJ, Ying LM, Klenerman D. Trapping of proteins under physiological conditions in a nanopipette. Angew Chem Int Ed Engl. 2005; 44:3747–3750. [PubMed: 15883978]
66. Clarke RW, Piper JD, Ying L, Klenerman D. Surface conductivity of biological macromolecules measured by nanopipette dielectrophoresis. Phys Rev Lett. 2007:98.
67. Gong JR. Label-free attomolar detection of proteins using integrated nanoelectronic and electrokinetic devices. Small. 2010; 6:967–973. [PubMed: 20209654]
68. Asokan SB, Jawerth L, Carroll RL, et al. Two-dimensional manipulation and orientation of actin-myosin systems with dielectrophoresis. Nano Lett. 2003; 3:431–437.
69. Maruyama H, Nakayama Y. Trapping protein molecules at a carbon nanotube tip using dielectrophoresis. Appl Phys Express. 2008; 1:124001-1–124001-3.
70. Castillo J, Tanzi S, Dimaki M, Svendsen W. Manipulation of self-assembly amyloid peptide nanotubes by dielectrophoresis. Electrophoresis. 2008; 29:5026–5032. [PubMed: 19130587]
71. Jones, TB. Electromechanics of Particles. Cambridge University; Cambridge, UK: 1995.
72. Gencoglu A, Camacho-Alanis F, Nguyen VT, et al. Quantification of pH gradients and implications in insulator-based dielectrophoresis of biomolecules. Electrophoresis. 2011; 32:2436–2447. [PubMed: 21874654]
73. Nakano A, Luo J, Ros A. Temporal and spatial temperature measurement in insulator-based dielectrophoretic devices. Anal Chem. 2014; 86:6516–6524. [PubMed: 24889741]
74. Oleinikova A, Sasisanker P, Weingartner H. What can really be learned from dielectric spectroscopy of protein solutions? A case study of ribonuclease A. J Phys Chem B. 2004; 108:8467–8474.
75. Mellor BL, Wood SJ, Mazzeo BA. Quantitation of pH-induced aggregation in binary protein mixtures by dielectric spectroscopy. Protein J. 2012; 31:703–709. [PubMed: 23001617]
76. Lisdat F, Schaefer D. The use of electrochemical impedance spectroscopy for biosensing. Analyt Bioanal Chem. 2008; 39167:1555–15. [PubMed: 18414837]
77. Bard, AJ. Electrochemical Methods: Fundamentals and Applications. 2nd. John Wiley & Sons, Inc; NJ, USA: 2001.
78. Gomes WP, Vanmaekelbergh D. Impedance spectroscopy at semiconductor electrodes: Review and recent developments. Electrochim Acta. 1996; 41:967–973.
79. Bisquert J, Fabregat-Santiago F, Mora-Sero I, et al. A review of recent results on electrochemical determination of the density of electronic states of nanostructured metal-oxide semiconductors and organic hole conductors. Inorgan Chim Acta. 2008; 361:684–698.
80. Nechache A, Cassir M, Ringuede A. Solid oxide electrolysis cell analysis by means of electrochemical impedance spectroscopy: a review. J Power Sources. 2014; 258:164–181.
81. Niya SMR, Hoorfar M. Study of proton exchange membrane fuel cells using electrochemical impedance spectroscopy technique: a review. J Power Sources. 2013; 240:281–293.
82. Rodrigues S, Munichandraiah N, Shukla AK. A review of state-of-charge indication of batteries by means of a.c impedance measurements. J Power Sources. 2000; 87:12–20.
83. Kokil A, Yang K, Kumar J. Techniques for characterization of charge carrier mobility in organic semiconductors. J Polym Sci Part B: Polym Phys. 2012; 504:1130–114.
84. Macdonald DD. Reflections on the history of electrochemical impedance spectroscopy. Electrochim Acta. 2006; 51:1376–1388.
85. Huang VM, Wu SL, Orazem ME, et al. Local electrochemical impedance spectroscopy: a review and some recent developments. Electrochim Acta. 2011; 56:8048–8057.

86. Chang BY, Park SM. Electrochemical impedance spectroscopy. Annu Rev Anal Chem. 2010; 3:207–229.

87. Schichlein H, Muller AC, Voigts M, Krugel A, Ivers-Tiffee E. Deconvolution of electrochemical impedance spectra for the identification of electrode reaction mechanisms in solid oxide fuel cells. J Appl Electrochem. 2002; 32:875–882.

88. Jensen SH, Hauch A, Hendriksen PV, et al. A method to separate process contributions in impedance spectra by variation of test conditions. J Electrochem Soc. 2007; 154:B1325–B1330.

89. Jubery TZ, Srivastava SK, Dutta P. Dielectrophoretic separation of bioparticles in microdevices: a review. Electrophoresis. 2014; 35:691–713. [PubMed: 24338825]

90. Hollingsworth AD, Saville DA. A broad frequency range dielectric spectrometer for colloidal suspensions: cell design, calibration, and validation. J Coll Interface Sci. 2003; 257:65–76.

91. Hollingsworth AD, Saville DA. Dielectric spectroscopy and electrophoretic mobility measurements interpreted with the standard electrokinetic model. J Coll Interface Sci. 2004; 272:235–245.

92. Russell AS, Scales PJ. Insights into sample preparation for dielectric response measurements. Colloids Surf A: Physicochem Eng Aspects. 2001; 194:271–286.

93. Zhao Y, Wang M, Hammond RB. Characterisation of nano-particles in colloids: relationship between particle size and electrical impedance spectra. J Nanosci Nanotechnol. 2013; 13:808–812. [PubMed: 23646520]

94•. Zhao H. Double-layer polarization of a non-conducting particle in an alternating current field with applications to dielectrophoresis. Electrophoresis. 2011; 32(17):2232–2244. Review paper related to polarization mechanisms of particles for DEP applications. [PubMed: 21823130]

95. Zhao H, Bau HH. Effect of double-layer polarization on the forces that act on a nanosized cylindrical particle in an ac electrical field. Langmuir. 2008; 24:6050–6059. [PubMed: 18476669]

96. Saville DA, Bellini T, Degiorgio V, Mantegazza F. An extended Maxwell–Wagner theory for the electric birefringence of charged colloids. J Chem Phys. 2000; 113:6974–6983.

97. Obrien RW. The high-frequency dielectric-dispersion of a colloid. J Coll Interface Sci. 1986; 113:81–93.

98. Dukhin, SS.; Shilov, VN. Dielectric Phenomena and the Double-Layer in Disperse Systems and Polyelectrolytes. Wiley; NY, USA: 1974.

99. Zhao K, He K. Dielectric relaxation of suspensions of nanoscale particles surrounded by a thick electric double layer. Phys Rev B. 2006; 74:205319-1–205319-10.

100. Zhao H, Bau HH. Polarization of nanorods submerged in an electrolyte solution and subjected to an ac electrical field. Langmuir. 2010; 26(8):5412–5420. [PubMed: 20039656]

101. Zhao H, Bau HH. The polarization of a nanoparticle surrounded by a thick electric double layer. J Coll Interface Sci. 2009; 333:663–671.

102. Zhou H, Preston MA, Tilton RD, White LR. Calculation of the electric polarizability of a charged spherical dielectric particle by the theory of colloidal electrokinetics. J Coll Interface Sci. 2005; 285:845–856.

103. Feldman Y, Ermolina I, Hayashi Y. Time domain dielectric spectroscopy study of biological systems. IEEE Trans Dielectrics Electrical Insulation. 2003; 5:728–753.

104. Roland CM. Characteristic relaxation times and their invariance to thermodynamic conditions. Soft Matter. 2008; 4:2316–2322.

105. Asami K. Characterization of biological cells by dielectric spectroscopy. J Non-Crystalline Solids. 2002; 305:268–277.

106. Cametti C, Marchetti S, Gambi CMC, Onori G. Dielectric relaxation spectroscopy of lysozyme aqueous solutions: analysis of the delta-dispersion and the contribution of the hydration water. J Phys Chem B. 2011; 115:7144–7153. [PubMed: 21557554]

107. Schlecht P, Mayer A, Hettner G, Vogel H. Dielectric properties of hemo globin and myo globin part 1. Influence of solvent and particle size on the dielectric dispersion. Biopolymers. 1969; 7:963–974.

108. Wolf M, Gulich R, Lunkenheimer P, Loidl A. Relaxation dynamics of a protein solution investigated by dielectric spectroscopy. Biochim Biophys Acta. 2012; 1824:723–730. [PubMed: 22406314]
109. Haggis GH, Buchanan TJ, Hasted JB. Estimation of protein hydration by dielectric measurements at microwave frequencies. Nature. 1951; 167:607–608. [PubMed: 14826872]
110. Buchanan TJ, Haggis GH, Hasted JB, Robinson BG. The dielectric estimation of protein hydration. Proc R Soc London Ser A. 1952; 213:379–391.
111. Pennock BE, Schwan HP. Further observations on electrical properties of hemoglobin-bound water. J Phys Chem. 1969; 73:2600–2610. [PubMed: 5798200]
112. Yokoyama K, Kamei T, Minami H, Suzuki M. Hydration study of globular proteins by microwave dielectric spectroscopy. J Phys Chem B. 2001; 105:12622–12627.
113. Pethig R. Protein-water interactions determined by dielectric methods. Annu Rev Phys Chem. 1992; 43:177–205. [PubMed: 1463572]
114. Oncley JL. The investigation of proteins by dielectric measurements. Chem Rev. 1942; 30:433–450.
115. Richert, R.; Blumen, A. Disorder Effects On Relaxational Processes: Glases, Polymers, Proteins. Springer; Berlin, Germany: 1994.
116. Demchenko AP. Dielectric behavior of proteins. J Mol Liquids. 1993; 56:127–139.
117. Nandi N, Bagchi B. Anomalous dielectric relaxation of aqueous protein solutions. J Phys Chem A. 1998; 102:8217–8221.
118. Yada H, Nagai M, Tanaka K. The intermolecular stretching vibration mode in water isotopes investigated with broadband terahertz time-domain spectroscopy. Chem Phys Lett. 2009; 473:279–283.
119. Matyushov DV. On the theory of dielectric spectroscopy of protein solutions. J Phys Condens Matter. 2012; 24:2–8.
120. Gunda NSK, Mitra SK. Modeling of dielectrophoretic transport of myoglobin molecules in microchannels. Biomicrofluidics. 2010; 4:014105-1–014105-20.
121. Martinez-Duarte R, Camacho-Alanis F, Renaud P, Ros A. Dielectrophoresis of lambda-DNA using 3D carbon electrodes. Electrophoresis. 2013; 34:1113–1122. [PubMed: 23348619]
122. Gan L, Chao TC, Camacho-Alanis F, Ros A. Six-helix bundle and triangle DNA origami insulator-based dielectrophoresis. Anal Chem. 2013; 85:11427–11434. [PubMed: 24156514]
123. Lapizco-Encinas BH, Simmons BA, Cummings EB, Fintschenko Y. Dielectrophoretic concentration and separation of live and dead bacteria in an array of insulators. Anal Chem. 2004; 76:1571–1579. [PubMed: 15018553]
124. Elitas M, Martinez-Duarte R, Dhar N, McKinney JD, Renaud P. Dielectrophoresis-based purification of antibiotic-treated bacterial subpopulations. Lab Chip. 2014; 14:1850–1857. [PubMed: 24756475]
125. Roy S, Richert R. Dielectric spectroscopy study of myoglobin in glycerol-water mixtures. Biochim Biophys Acta. 2014; 1844:323–329. [PubMed: 24291287]
126. Jansson H, Bergman R, Swenson J. Role of Solvent for the dynamics and the glass transition of proteins. J Phys Chem B. 2011; 115:4099–4109. [PubMed: 21425816]
127. Kyritsis A, Panagopoulou A, Pissis P, et al. Water and protein dynamics in protein-water mixtures over wide range of composition IEEE transactions on dielectrics and electrical insulation. Roser Sabater i Serra. 2012; 19:1239–1246.
128. Mazzeo BA, Flewitt AJ. Observation of protein-protein interaction by dielectric relaxation spectroscopy of protein solutions for biosensor application. Appl Phys Lett. 2007; 90:123901-1–123901-3.
129. Mellor BL, Cortes EC, Khadka S, Mazzeo BA. Increased bandwidth for dielectric spectroscopy of proteins through electrode surface preparation. Rev Sci Instrum. 2012; 83:015110-1–015110-6. [PubMed: 22299989]
130. Ben Ishai P, Talary MS, Caduff A, Levy E, Feldman Y. Electrode polarization in dielectric measurements: a review. Meas Sci Technol. 2013:1–21.

131. Schwan HP. Electrode polarization impedance and measurements in biological material. Ann NY Acad Sci. 1968; 148:191. [PubMed: 5237641]

132. Malleo D, Nevill JT, van Ooyen A, et al. Note: characterization of electrode materials for dielectric spectroscopy. Rev Sci Instrum. 2010; 81:016104-1–016104-3. [PubMed: 20113135]

133. Zhang K, Hu Z, Chen J. Functional porous carbon-based composite electrode materials for lithium secondary batteries. J Energy Chem. 2013; 22:214–225.

134. Zaidi SA. Graphene: a comprehensive review on its utilization in carbon paste electrodes for improved sensor performances. Int J Electrochem Sci. 2013; 8:11337–11355.

135. Martinez-Duarte R, Renaud P, Madou MJ. A novel approach to dielectrophoresis using carbon electrodes. Electrophoresis. 2011; 32:2385–2392. [PubMed: 21792991]

136. Shafee H, Caldwell JL, Sano MB, Davalos RV. Contactless dielectrophoresis: a new technique for cell manipulation. Biomed Microdevices. 2009; 11:997–1006. [PubMed: 19415498]

137. Shafiee H, Sano MB, Henslee EA, Caldwell JL, Davalos RV. Selective isolation of live/dead cells using contactless dielectrophoresis (cDEP). Lab Chip. 2010; 10:438–445. [PubMed: 20126683]

138∂. Davalos, VR.; Simmons, BA.; Crocker, RW.; Cummings, EB. Insulator-based DEP with impedance measurements for analyte detection. Corporation S; USA: 2010. p. 1-10.Patent incorporating impedance measurements in an insulator-based dielectrophoresis device

139. Camacho-Alanis F, Castaneda H, Zangari G, Swami NS. Electrochemical impedance study of GaAs surface charge modulation through the deprotonation of carboxylic acid monolayers. Langmuir. 2011; 27:11273–11277. [PubMed: 21859118]

140. Wu LL, Camacho-Alanis F, Castaneda H, Zangari G, Swami N. Electrochemical impedance spectroscopy of carboxylic-acid terminal alkanethiol self assembled monolayers on GaAs substrates. Electrochim Acta. 2010; 55:8758–8765.

141. Mazzeo BA, Flewitt AJ. Two- and four-electrode, wide-bandwidth, dielectric spectrometer for conductive liquids: theory, limitations, and experiment. J Appl Phys. 2007:104106-1–104106-6.

142. Mazzeo BA, Chandra S, Mellor BL, Arellano J. Temperature-stable parallel-plate dielectric cell for broadband liquid impedance measurements. Rev Sci Instrum. 2010; 81:125103-1–125103-5. [PubMed: 21198047]

143. Krishnan R, Sullivan BD, Mifflin RL, Esener SC, Heller MJ. Alternating current electrokinetic separation and detection of DNA nanoparticles in high-conductance solutions. Electrophoresis. 2008; 29:1765–1774. [PubMed: 18393345]

144. Krishnan R, Dehlinger DA, Gemmen GJ, et al. Interaction of nanoparticles at the DEP microelectrode interface under high conductance conditions. Electrochem Commun. 2009; 11:1661–1666. [PubMed: 20160949]

145. Gallo-Villanueva RC, Sano MB, Lapizco-Encinas BH, Davalos RV. Joule heating effects on particle immobilization in insulator-based dielectrophoretic devices. Electrophoresis. 2014; 35:352–361. [PubMed: 24002905]

146. Gagnon ZR. Cellular dielectrophoresis: applications to the characterization, manipulation, separation and patterning of cells. Electrophoresis. 2011; 32:2466–2487. [PubMed: 21922493]

147. Martinez-Duarte R, Gorkin RA III, Abi-Samra K, Madou MJ. The integration of 3D carbon-electrode dielectrophoresis on a CD-like centrifugal microfluidic platform. Lab Chip. 2010; 10:1030–1043. [PubMed: 20358111]

148. Demierre N, Braschler T, Linderholm P, et al. Characterization and optimization of liquid electrodes for lateral dielectrophoresis. Lab Chip. 2007; 7:355–365. [PubMed: 17330167]

149. Demierre N, Braschler T, Muller R, Renaud P. Focusing and continuous separation of cells in a microfluidic device using lateral dielectrophoresis. Sens Actuators B Chem. 2008; 132:388–396.

Key terms

Dielectrophoresis: Technique used to separate, concentrate and fractionate biomolecules in electric field gradients.

Electrochemical impedance spectroscopy: Electrochemical technique that measures the impedance of samples.

Dielectric spectroscopy: Technique that measures the dielectric properties of materials. It uses the same information obtained by electrochemical impedance spectroscopy but differs in its analysis and approach to data representation.

Electrode polarization: Electrochemical phenomenon that takes place at the interface between the electrode and ion-containing liquid.

Executive summary

Advances in protein of dielectrophoresis

- Dielectrophoresis (DEP) is a powerful technique for future fractionation, purification and concentration of proteins.
- Several DEP properties of proteins have been determined as shown in Table 1.
- One major problem in this field is that the origin of protein DEP is still not well understood, which is essential for future protein manipulation.

Electrochemical impedance spectroscopy & dielectric spectroscopy measurements

- Electrochemical impedance spectroscopy (EIS) and dielectric spectroscopy (DS) measurements are suitable for DEP studies of proteins since the technique is a label-free method and can access the polarizability of proteins, and hence, their DEP behavior can be predicted.
- EIS and DS measurements have to be combined with suitable models such as Maxwell–Wagner, Dukhin–Shilov or Poisson–Nernst–Planck models, to be able to determine the polarization of proteins.
- Electrode Polarization (EP) is one of the main challenges to perform EIS and DS measurements at low frequencies although there are several alternatives to mitigate this effect.
- Microfluidic and nanofabricated DEP devices may be used to integrate EIS and DS in protein DEP studies.

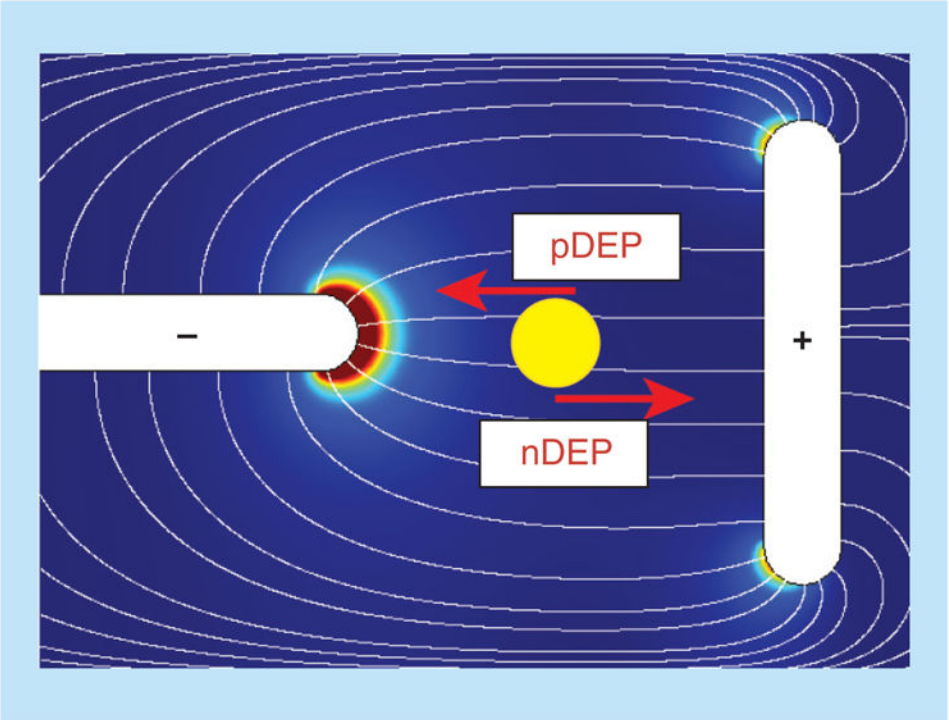

Figure 1. A polarizable particle in a nonuniform electric field

The highest electric field gradient is located at the tip of the left electrode denoted. When a polarizable particle, represented by the yellow circle in the figure, is placed in the nonuniform electric field, depending on the permittivity of the medium and the particle, the particle can move toward (pDEP) or away (nDEP) from the high electric field gradient regions (color scale represented as heat map; red refers to high).

nDEP: Negative dielectrophoresis; pDEP: Pegative dielectrophoresis.

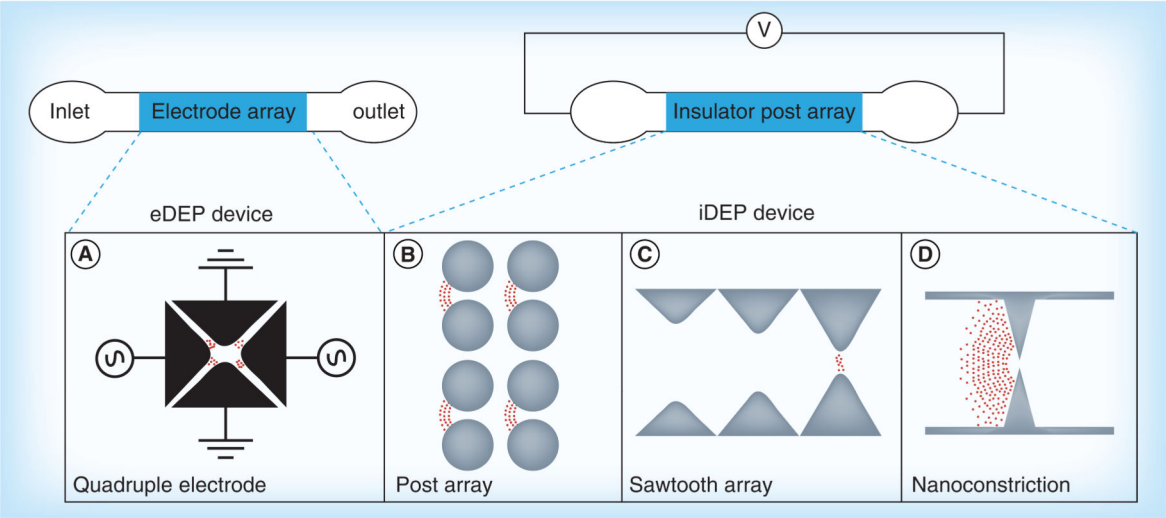

Figure 2. Depiction of experimental devices used to study protein dielectrophoresis

(A) eDEP device: a quadruple electrode geometry is shown exemplarily for an eDEP device as utilized in Bakewell *et al*. [13,14] to manipulate proteins under AC conditions. Red dots at the edges of the electrodes represent proteins trapped in positive dielectrophoresis regions where the electric field gradient is highest. Black color indicates microelectrodes. **(B–D)** show iDEP approaches where gray indicates the insulating material. **(B)** A circular insulating post-array as utilized by Lapizco-Encinas *et al*. [4]. Under DC conditions, the protein bovine serum albumin is repelled from the constrictions where the electric field gradient is highest, indicating negative dielectrophoresis. **(C)** Insulating constrictions with sawtooth shapes realized by Staton *et al*. [44]. With the application of a DC voltage, β-amyloid fibrils are trapped at the narrow constrictions by positive dielectrophoresis. **(D)** A nanoconstriction insulating device used in [15,16]. With the application of an appropriate AC voltage as well as a DC bias, proteins are accumulated continuously due to negative dielectrophoresis.

eDEP: Electrode-based dielectrophoresis; iDEP: Insulator-based dielectrophoresis.

Adapted with permission from [31] WILEY-VCH Verlag GmbH & Co. KGaA, Weinheim (2013).

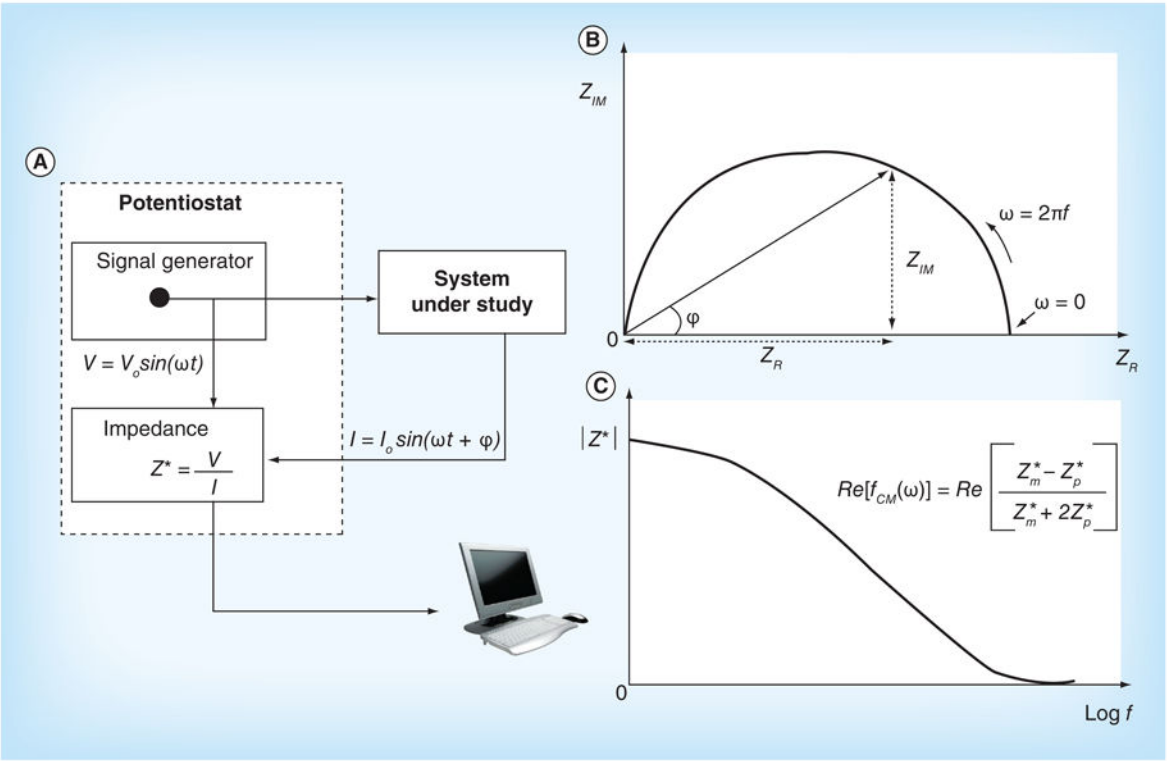

Figure 3. Electrochemical impedance spectroscopy measurements and its graphical representations

(A) Representation of electrochemical impedance spectroscopy measurements: an AC potential (perturbation) is applied to the system under study. The total impedance is measured in relation to the applied potential and the current response. **(B)** Nyquist plot: the imaginary part of the impedance is plotted against the real part of the impedance. Note that the frequency increases from right to left. **(C)** Bode plot: the magnitude of the total impedance *Z** is plotted against the frequency.

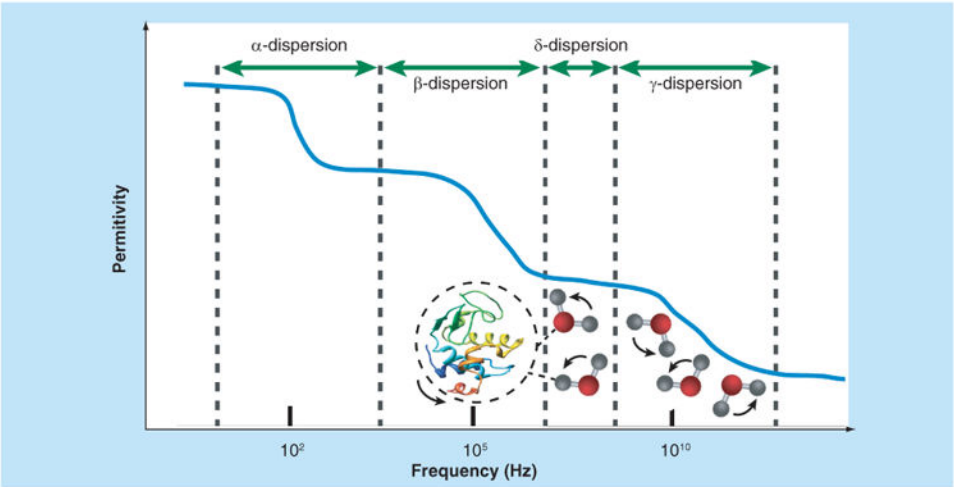

Figure 4. Complex permittivity spectrum of a typical protein solution showing distinct dispersions at their respective frequency range

The plot shows the contributions of the β-, δ- and γ-dispersions, which arise from reorientation motions of protein molecules and the bound and the free water molecules, respectively. α-dispersions are usually associated with diffusion processes of ionic species. Adapted with permission from [35] [© Elsevier (2013); and [108] [© Elsevier (2012).

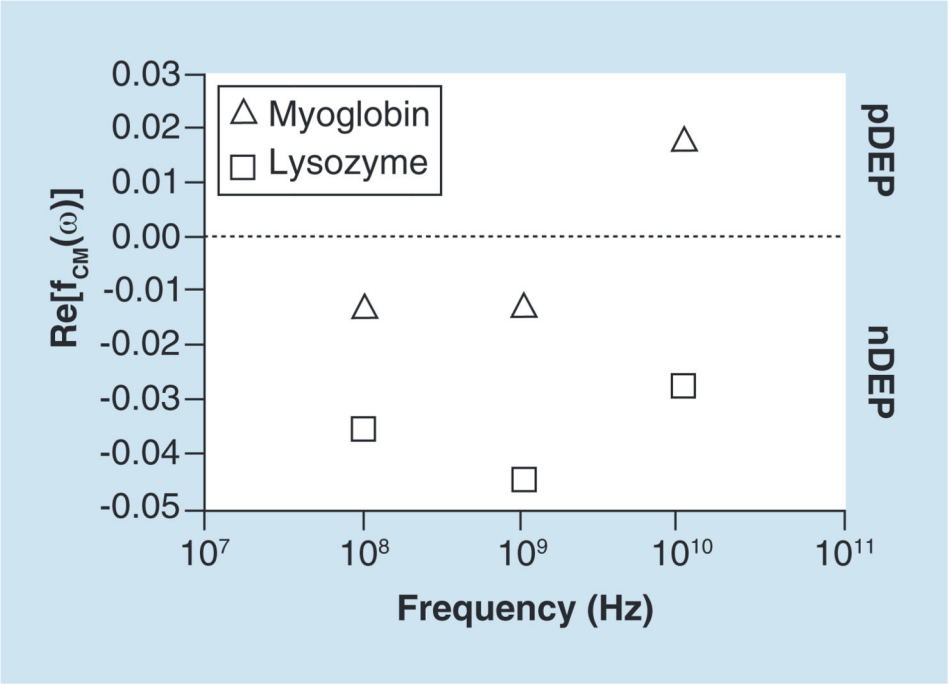

Figure 5. Calculation of Re[$f_{CM}(\omega)$] using Equation 1

Dielectric spectra of myoglobin and lysozyme were obtained from [117] and [106], respectively, the dielectric spectrum of water was taken from [118]. According to the calculations, nDEP behavior is expected for lysozyme while a crossover frequency from nDEP to pDEP is expected for myoglobin at high frequencies. Concentration of myoglobin and lysozyme is 170 and 110 mg/ml, respectively, and measurements were performed at room temperature.

nDEP: Negative dielectrophoresis; pDEP: Positive dielectrophoresis.

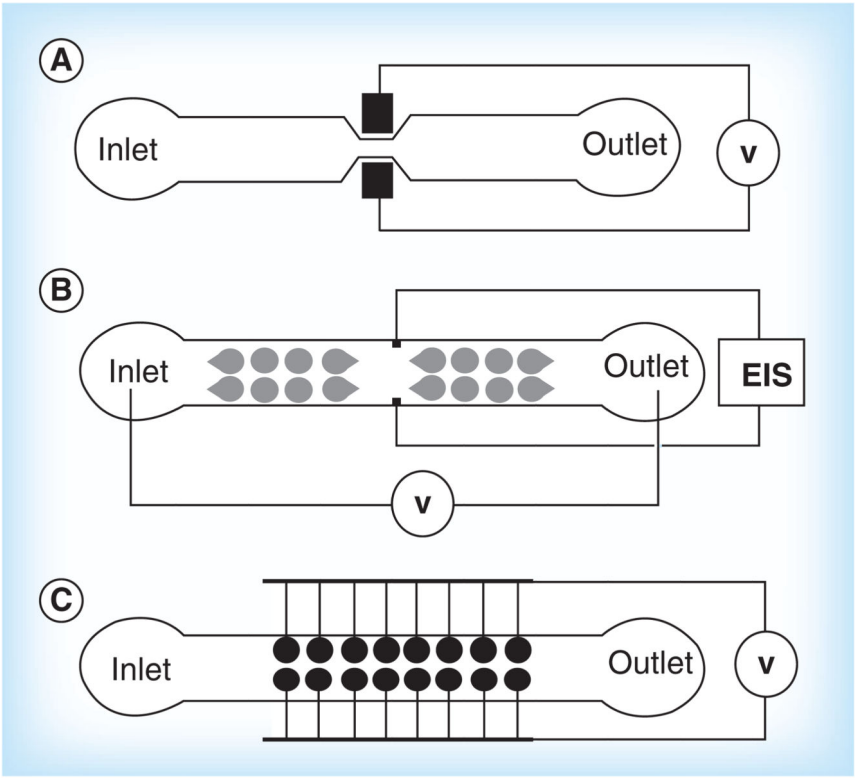

Figure 6. Potential microfluidic devices for electrochemical impedance spectroscopy/dielectric spectroscopy measurements

(A) Contactless dielectrophoresis (cDEP) device utilized in [136]. cDEP is an extension of an insulator-based dielectrophoresis (iDEP) device with the characteristic that the electrodes are located outside of the main microfluidic channel eliminating undesired electrode reactions or electrode polarization effects. **(B)** Microfluidic device utilized in [138]. iDEP is used to trapp cells while electrodes located next to the walls are used as sensors performing EIS measurements. **(C)** A carbon-dielectrophoresis device utilized in [135]. Carbon-dielectrophoresis is a combination of iDEP and eDEP. Posts in the microfluidic device are patterned and then carbonized making the material conductive.

EIS: Electrochemical impedance spectroscopy.

Table 1

Dielectrophoresis behavior of different proteins and peptides from experimental results

Proteins used	DEP behavior	Ref.
Avidin	pDEP @ <9 MHz, nDEP >9 MHz	[13,64]
Concanavalin	pDEP @ 1 MHz	[64]
Ribonuclease A	pDEP @ 1 MHz	[64]
Yellow fluorescence protein	pDEP @ DC conditions	[65,66]
R-phycoerythrin	pDEP @ 100 kHz, 1 MHz	[10,49]
BSA	pDEP @ DC and 200 kHz/nDEP @DC	[2,9,14]/[4]
Aβ amyloid	pDEP @ DC conditions	[44]
PSA	pDEP @ 47 Hz	[67]
IgG	pDEP @ DC and low Freq.	[2,11,46]
Actin	pDEP @ 2 MHz	[68]
Streptavidin	pDEP @ 10 KHz; nDEP @ 1 MHz	[16,69]
Amyloid peptide nanotubes	pDEP @ 1 MHz	[70]
β-Galactosidase	nDEP @ DC and low Freq.	[11,47]
Neuropeptide Y	nDEP @ 3 MHz	[51]

BSA: Bovine serum albumin; DEP: Dielectrophoresis; nDEP: Negative dielectrophoresis; pDEP: Positive dielectrophoresis.